doi:10.1016/j.jmb.2006.03.068 J. Mol. Biol. (2006) 359, 1097–1106

JMB

Available online at www.sciencedirect.com

SCIENCE DIRECT®

ELSEVIER

Quantitative Analysis of Multi-component Spherical Virus Assembly: Scaffolding Protein Contributes to the Global Stability of Phage P22 Procapsids

Kristin N. Parent[1], Adam Zlotnick[2] and Carolyn M. Teschke[1]*

[1]*Department of Molecular and Cell Biology, University of Connecticut, Storrs, CT 06269-3125, USA*

[2]*The University of Oklahoma Health Sciences Center Department of Biochemistry and Molecular Biology Oklahoma City, OK 73190 USA*

**Corresponding author*

Assembly of the hundreds of subunits required to form an icosahedral virus must proceed with exquisite fidelity, and is a paradigm for the self-organization of complex macromolecular structures. However, the mechanism for capsid assembly is not completely understood for any virus. Here we have investigated the *in vitro* assembly of phage P22 procapsids using a quantitative model specifically developed to analyze assembly of spherical viruses. Phage P22 procapsids are the product of the co-assembly of 420 molecules of coat protein and ~100–300 molecules of scaffolding protein. Scaffolding protein serves as an assembly chaperone and is not part of the final mature capsid, but is essential for proper procapsid assembly. Here we show that scaffolding protein also affects the thermodynamics of assembly, and for the first time this quantitative analysis has been performed on a virus composed of more than one type of protein subunit. Purified coat and scaffolding proteins were mixed in varying ratios *in vitro* to form procapsids. The reactions were allowed to reach equilibrium and the proportion of the input protein assembled into procapsids or remaining as free subunits was determined by size exclusion chromatography and SDS-PAGE. The results were used to calculate the free energy contributions for individual coat and scaffolding proteins. Each coat protein subunit was found to contribute $-7.2(\pm 0.1)$ kcal/mol and each scaffolding protein $-6.1(\pm 0.2)$ kcal/mol to the stability of the procapsid. Because each protein interacts with two or more neighbors, the pair-wise energies are even less. The weak protein interactions observed in the assembly of procapsids are likely important in the control of nucleation, since an increase in affinity between coat and scaffolding proteins can lead to kinetic traps caused by the formation of too many nuclei. In addition, we find that adjusting the molar ratio of scaffolding to coat protein can alter the assembly product. When the scaffolding protein concentration is low relative to coat protein, there is a correspondingly low yield of proper procapsids. When the relative concentration is very high, too many nuclei form, leading to kinetically trapped assembly intermediates.

Keywords: subunit interactions; dissociation constant; energetics; phage assembly; bacteriophage

Introduction

The amino acid sequence of capsid subunits must contain information not only about the structure of the subunits but also about the self-assembly process. While some viruses assemble from small preformed oligomers of their coat proteins, other viruses such as phage P22 and herpesvirus assemble from monomeric proteins.[1–4] The process of subunit assembly is strictly controlled through protein–protein interactions such that icosahedral structures are formed, rather than aberrant non-icosahedral structures. Weak protein–protein interactions through polyvalent subunits have been

Abbreviations used: SEC, size exclusion chromatography; CCMV, cowpea chlorotic mottle virus; HBV, hepatitis B virus.

E-mail address of the corresponding author: teschke@uconn.edu

suggested to be the driving force for virus assembly.[5–7] These weak subunit associations allow for thermodynamic editing during the assembly process, whereas high affinity interactions are predicted[8–11] and have been shown[12,13] to lead to kinetic trapping of assembly intermediates or off-pathway products. Detailed analysis of the binding affinities of capsid subunits has been done with cowpea chlorotic mottle virus (CCMV) and hepatitis B virus (HBV), both of which have capsids comprised of a single capsid protein that forms a stable dimer. Both show capsid subunit binding interactions of approximately -7 kcal/mol per capsid protein dimer.[5,14] Here, we investigate the interactions involved in capsid assembly for the procapsid of the $T=7$ *Salmonella* bacteriophage P22, a capsid comprised of coat and scaffolding proteins, to understand the energetics of the interactions in this more complex macromolecular assembly.

The morphogenic pathway of phage P22 involves the co-assembly of 420 molecules of coat protein (product of gene *5*; gp5) with ~100–300 molecules of scaffolding protein (product of gene *8*) in a nucleation-limited reaction. Some minor proteins (products of genes *7*, *16* and *20*, referred to as injection proteins) and the portal protein complex (product of gene *1*) are also incorporated during assembly.[15,16] Scaffolding protein directs the assembly of the procapsid. Without scaffolding protein, coat protein assembles into $T=4$ capsids and aberrant spiral structures that have their fivefold and sixfold vertices located inappropriately so that closed procapsid structures do not form. The formation of these misassembled structures occurs only at relatively high coat protein concentrations.[17,18] The number of scaffolding protein molecules in a procapsid varies from about 100 to 300 molecules, depending on the conditions of assembly.[19,20] The minor injection proteins are incorporated early in assembly[21–23] also through interactions with scaffolding protein.[24] The double-stranded (ds) DNA is actively packaged into the procapsid through the unique portal vertex.[25] Concomitant with DNA packaging, scaffolding protein exits from the procapsid to take part in additional rounds of assembly, and the capsid matures.[26,27] The dsDNA is stabilized by the addition of proteins that close the portal vertex, and finally tailspikes, the cell recognition and attachment proteins, are added. In the processes of folding and assembly, none of the proteins are covalently modified or proteolyzed.[28]

An important advantage of phage P22 as an assembly model is the simplicity of the system. The proteins needed for assembly of P22 procapsids can all be purified and are active for assembly.[29] *In vitro*, only coat and scaffolding proteins are required to assemble a procapsid-like particle, which we will refer to as a procapsid.[4,30] The *in vitro* assembled procapsid has the same morphology and size as the *in vivo* generated procapsid.[4] Because of the relative simplicity of the reaction, we can manipulate the outcome; we recently showed that changing the composition of the buffer alters the product of assembly.[12] When the anion concentration in the buffer is low, then too many nuclei form and assembly is trapped in a partially assembled state, which we call partial capsids. We proposed that the affinity between coat and scaffolding proteins is too high in these buffer conditions.

While there is a plethora of general information on the assembly of phage P22, the only rigorous thermodynamic analysis of *in vitro* assembly was based on a model of assembly of filamentous proteins.[31] For filamentous protein assembly, where there is one nucleus for a very long polymer, the process of slow nucleation followed by growth of the large polymer leads to the observed sigmoidal assembly kinetics.[32] For an icosahedral particle, where there are at most a few hundred subunits, the observed sigmoidal assembly reaction kinetics result from the time it takes to achieve a steady state concentration of assembly intermediates rather than very slow nucleation.[8] Thus, the analysis of capsid assembly reactions must differ from that of filamentous protein assembly.[33]

Zlotnick's group has recently established a generalized, thermodynamically rigorous model to describe the assembly of icosahedral viruses.[9,33,34] These models have been used in the characterization of the assembly of HBV,[5,9] CCMV[35] and papillomavirus.[36] Essentially, assembly is described in terms of a cascade of reactions. Though the overall reaction can be expressed in terms of a simple mass action law (see equations (1)–(3)), cascades can have distinctly complex behavior. While assembly reactions rapidly reach equilibrium, dissociation of spherical assemblies is impeded by a large, kinetically derived energy barrier. This hysteresis arises from the rate of removing multivalent subunits from such complexes compared to the rate with which a free subunit will bind to a multivalent site. The assembly of HBV,[5,9] CCMV[35] requires only one protein species and is accurately described by the virus-specific model. Here, we expand the use of this model to the assembly of P22 procapsids and find that each subunit contact is weak but when the many contacts required to form a procapsid are combined, the result is a globally stable structure.

Results

Analysis of procapsid assembly reactions at equilibrium

In this study, we have determined the contributions of coat and scaffolding proteins to the stability of phage P22 procapsids based on a virus-specific thermodynamic–kinetic model.[8,34] Because the geometry of subunit interactions is not well defined for P22, we can only determine the per subunit association energy. The equilibrium

expression for the formation of a procapsid is:

$$420 \text{ coat protein} + Z \text{ scaffolding protein} \Leftrightarrow \text{procapsid} \quad (1)$$

Here the Z indicates that the number of scaffolding proteins incorporated varies with assembly conditions, especially total [scaffolding protein]. Then, the equilibrium constant for procapsid formation (K_{PC}) is:

$$K_{PC} = \frac{[PC]}{[coat]^{420}[scaffolding]^{Z}} \quad (2)$$

$$\log K_{PC} = \log[PC] - 420 \log[coat] - Z \log[scaffolding] \quad (3)$$

Because of the magnitude of K_{PC}, it is more convenient to work with the logarithmic form of the mass action law. $\log K_{PC}$ can be calculated because all of the concentrations on the right side of the equation can be determined. Because the number of coat proteins in a procapsid is absolute, it is simple to determine the concentration of procapsids assembled based on the amount of coat protein in the procapsid peak in a size exclusion chromatography (SEC) experiment (see Figure 1(a)). From the concentration of procapsids, the number of scaffolding protein molecules per procapsid particle can be calculated.

A series of assembly reactions were done in 20 mM phosphate with 50 mM NaCl, conditions where complete procapsids are efficiently generated.[12] In a given series of reactions, we varied the total protein concentration but held constant the ratio of scaffolding:coat protein. After equilibrium was reached (>20 h), the unassembled coat and scaffolding proteins were separated from procapsids by SEC (Figure 1). An aliquot of each fraction was run on SDS-polyacylamide gels and silver stained (Figure 1(a)). Shown in Figure 1(a) is an example of the separation achieved in the column chromatography under conditions with the highest protein concentrations. The amount of coat protein and scaffolding protein in each fraction was calculated from densitometric scans of the gels (Figure 1(b)). Any material observed between the procapsid and monomer peaks (less than ~5% of the total at the highest protein concentration) was simply divided between them; there is no evidence that assembly intermediates persist in reactions at equilibrium under these experimental conditions.[12] From these data, the concentration of coat and scaffolding proteins in procapsids and as soluble subunits were determined. Once the concentration of procapsids was determined, the number of scaffolding proteins per procapsid was calculated.

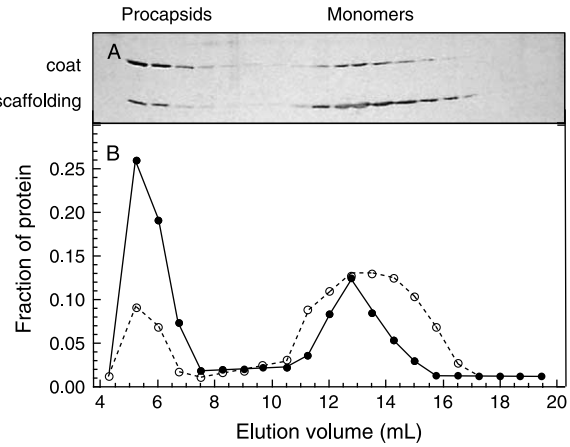

Figure 1. Analysis of assembly reactions. Coat and scaffolding proteins were mixed as described in Materials and Methods. After the reactions were incubated at 20 °C for at least 20 h, the reaction was applied to a size exclusion column. (a) A sample of each fraction was run on a SDS-gel and silver stained. (b) The amount of coat (filled circles) and scaffolding (open circles) proteins in each peak was determined by densitometry.

Isotherms showing that the concentration of coat protein assembled into procapsids varies with the input concentration of coat protein were generated from quantification of the assembly reactions. The concentration of procapsids *versus* input coat protein concentration for each scaffolding:coat protein ratio gives approximately the same slope of 0.00193 ± 0.0003 [procapsid] M/[coat protein] M for all ratios (Figure 2(a)). The addition of 1 mol of coat protein should give 1/420 mol of procapsids or 0.002 mol. Thus, the dependence of procapsid assembly on input coat protein concentration is exactly as anticipated.

At the three representative scaffolding:coat protein ratios shown in Figure 2(a), the data show the expected pseudo-critical concentration, or $K_{Dapparent}$, of ~5, 6.5 and 10.5 μM (see the arrows in Figure 2(a)). These agree qualitatively with older data where the pseudo-critical concentration for coat protein was determined to be ~6 μM at a single scaffolding protein concentration.[31] A pseudo-critical concentration derives from the extremely steep concentration dependence on coat protein for the procapsid assembly reaction, as described by the mass action law (equation (1)). In practical terms, above the $K_{Dapparent}$ value almost all of the additional coat protein in the initial reaction will go to form procapsids with a near constant amount of coat protein remaining when the reaction reaches equilibrium.

Though it is easily accessible experimentally, $K_{Dapparent}$ is a rigorously defined function of capsid stability and geometry.[8] A true critical concentration specifies that subunits freely equilibrate between two phases; $K_{Dapparent}$ is defined specifically for spherical oligomers because (i) free subunits will slowly increase with the total concentration of input coat protein, as predicted by equation (3), and (ii) hysteresis observed in the dissociation reaction of spherical oligomers will prevent the re-equilibration required for critical concentration phenomena.[8] This expected pseudo-

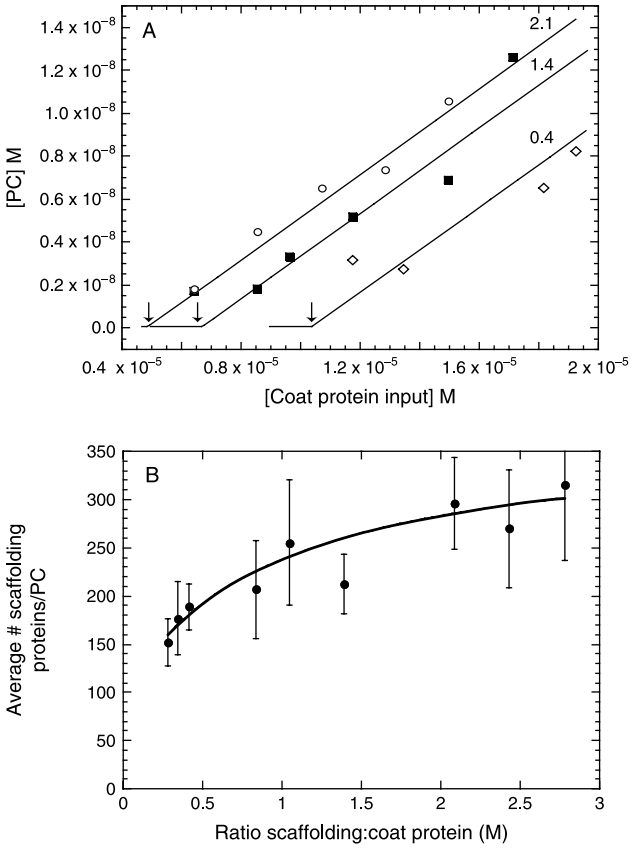

Figure 2. Characterization of assembly reactions. (a) Isotherms showing that the concentration of procapsids varies linearly with input coat protein concentration once the coat protein concentration is above the pseudo-critical concentration. Shown are the data from assembly reactions at three ratios of scaffolding:coat protein. The ratios are given above each data set. The arrows indicate the $K_{\mathrm{Dapparent}}$ value for coat protein at each input ratio. (b). The average number of scaffolding proteins incorporated into procapsids with increasing input ratio of scaffolding:coat protein. The line is the fit of the data with the formula for a rectangular hyperbola as described in Materials and Methods.

critical concentration ($K_{\mathrm{Dapparent}}$) has been observed not only for bacteriophage P22,[31,37] but also HBV[5] and CCMV.[13] In Figure 2(a) we observe for the first time that $K_{\mathrm{Dapparent}}$ is dependent on the proportion of scaffolding protein present in the reaction, which indicates that scaffolding contributes to procapsid stability.

The number of scaffolding proteins per procapsid was determined for each set of reactions performed at a particular molar ratio of scaffolding:coat protein. Shown in Figure 2(b), the number of scaffolding proteins per procapsid varied with the input scaffolding protein, as expected.[38,39] The data suggest that there is a lower limit to the number of scaffolding proteins needed to support assembly, and an upper limit to the number of protein binding sites within the $T=7$ capsid. Therefore, the data were fit to a rectangular hyperbola (line in Figure 2(b)), which gave a minimum of about 90 and a maximum of about 350 scaffolding protein subunits per procapsid at the limits of low and high scaffolding:coat protein ratios, respectively. This is in good agreement with previous work.[31,40,41]

Each coat or scaffolding protein subunit contributes only weakly to the stability of the procapsid

Assembly reactions were done with scaffolding: coat protein molar ratios from 0.28 to 2.8. For each reaction, the $\log K_{\mathrm{PC}}$ value was determined (equation (3)). In addition, an average $\log K_{\mathrm{PC}}$ was determined for all the reactions at each ratio. The $\log K_{\mathrm{PC}}$ is converted to ΔG_{PC} using:

$$\Delta G_{\mathrm{PC}} = -2.303RT \log K_{\mathrm{PC}} \qquad (4)$$

The contributions of scaffolding and coat proteins to procapsid stability were determined by plotting ΔG_{PC} *versus* the number of scaffold proteins per procapsid. These data readily fit to:

$$\Delta G_{\mathrm{PC}} = 420\Delta G_{\mathrm{coat}} + Z\Delta G_{\mathrm{scaffold}} \qquad (5)$$

where Z is the number of scaffolding proteins per procapsid. The linearity of the data strongly supports our analysis. This treatment yields an assessment of both ΔG_{coat} and $\Delta G_{\mathrm{scaffold}}$ under the condition of co-assembly while only making the assumption of thermodynamic linkage, i.e. that all proteins contribute to the overall procapsid stability.[9,34,42] Note that these are average values for association energy without reference to quasi-equivalence. In Figure 3(a), the ΔG_{PC} value is plotted against the number of scaffolding proteins per procapsid for each reaction. The fit of the data with equation (5) yielded a ΔG_{coat} of -7.2 ± 0.1 and a $\Delta G_{\mathrm{scaffold}}$ of -6.1 ± 0.2. These energies are equivalent to a dissociation constant of 5 μM for coat protein and 28 μM for scaffolding protein, and are consistent with estimates determined from different experiments.[6,41] Overall, coat protein contributes about -3000 kcal/mol to the stability of a procapsid and if the procapsid contains 300 scaffolding proteins, then scaffolding protein contributes about -1800 kcal/mol to procapsid stability.

Figure 3(a) shows the saturation of data on the plot of ΔG_{PC} *versus* scaffolding proteins/procapsid that we were able to achieve in these experiments. The ΔG_{PC} averaged over for an experimental series at a constant scaffolding:coat ratio (Figure 3(b)) gave ΔG values within the error of the values determined in Figure 3(a) and again show the scaffolding protein dependence on the stability of procapsids. Because the scaffolding and coat protein concentrations are in the range of their respective per subunit dissociation constants, the number of bound scaffolding proteins per capsid varies within an isotherm, contributing to the apparently large error bars in this plot.

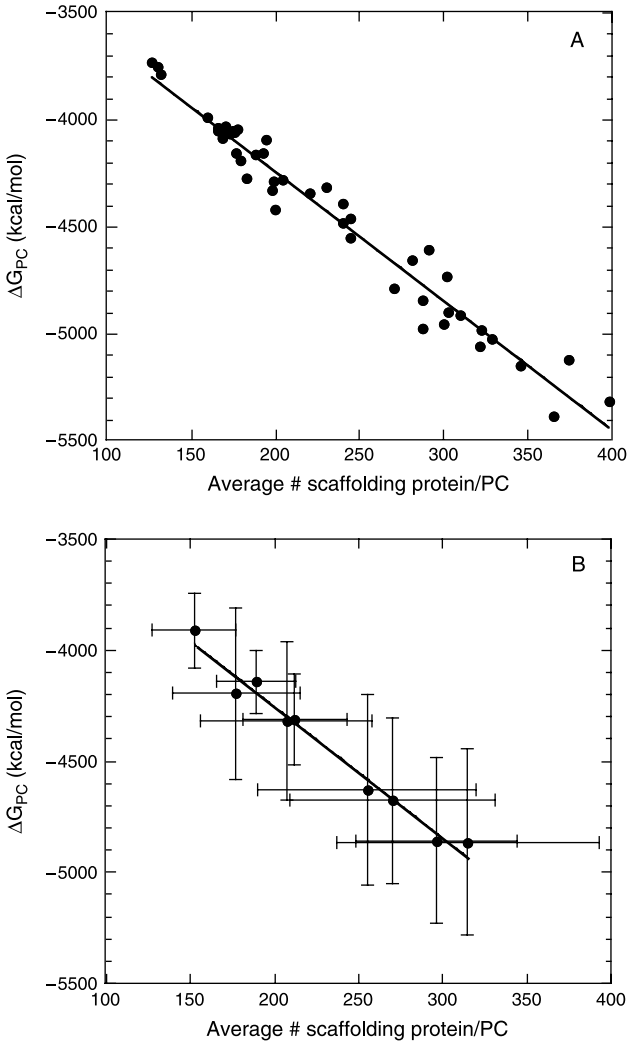

Figure 3. Contribution of scaffolding and coat proteins to the stability of procapsids. Assembly reactions were done at scaffolding protein to coat protein ratios of 0.28 to 2.8. SEC and SDS-PAGE were used to determine the incorporation of each protein into procapsids as shown in Figure 1. The ΔG_{PC} was calculated as described in the text. The data in both panels were fit with $\Delta G_{PC} = 420\Delta G_{coat} + Z\Delta G_{scaffold}$ (equation (5)). (a) The ΔG_{PC} value and number of scaffolding proteins per procapsid were determined for each reaction and represented by a single point on the plot. (b) The average for both ΔG_{PC} and the number of scaffolding proteins/procapsid at each particular input ratio of scaffolding:coat protein was determined and plotted with the error for both the ΔG_{PC} and number of scaffolding proteins/procapsid.

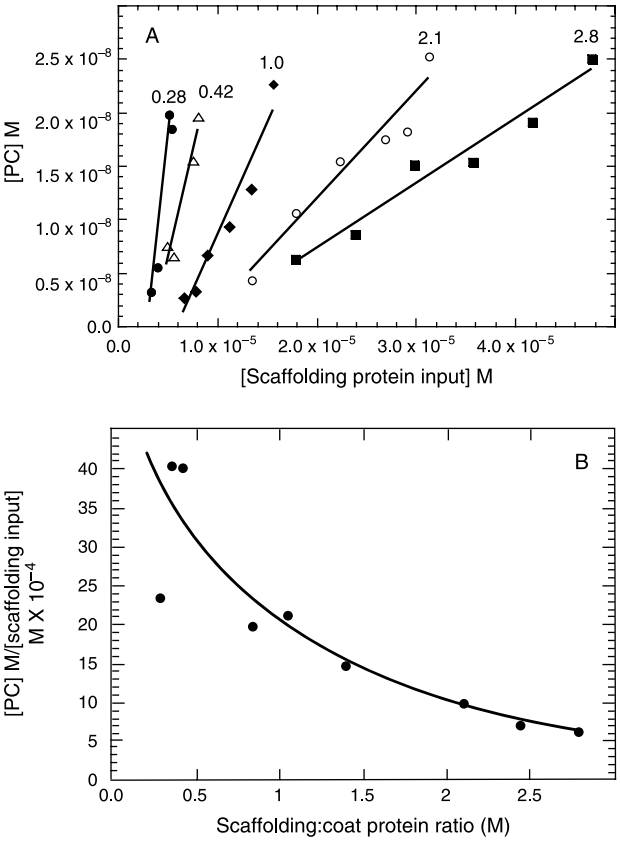

Figure 4. Dependence of procapsid assembly on input scaffolding protein concentration. (a) The concentration of procapsids generated for several scaffolding protein: input molar ratios, which are indicated by the number above each isotherm, is shown. The slopes of the lines were used to generate the plot shown in (b). In (b), the line is drawn to aid the eye and not meant to represent the fit of the data to any model.

There is an optimal range of scaffolding protein concentrations for procapsid assembly

The concentration of procapsids assembled in each reaction was plotted against the concentration of input scaffolding protein and organized by the input scaffolding:coat protein ratio (Figure 4(a)). At low input ratios, where scaffolding protein is limiting for assembly, increased concentrations of subunits directly yielded more procapsids. At higher input ratios, where scaffolding protein is in excess, the yield of the reactions became more dependent on the coat protein concentration, a dependence that is different from that seen when the data were plotted *versus* the input coat protein concentration (Figure 2(a)). The dependence of the slopes of the lines as a function of molar input ratio is shown in Figure 4(b). This plot shows that the dependence of the yield of procapsids on scaffolding protein decreases as the ratio of scaffolding:coat protein increases. These data suggest that the yield of procapsids should become close to zero at a high input ratio.

A high concentration of scaffolding protein inhibits assembly

Based on our previous work[12] and the data in Figure 4, we are led to the prediction that at very high scaffolding protein ratios, too many nuclei would form and ultimately inhibit assembly of procapsids. To test our prediction, we assembled

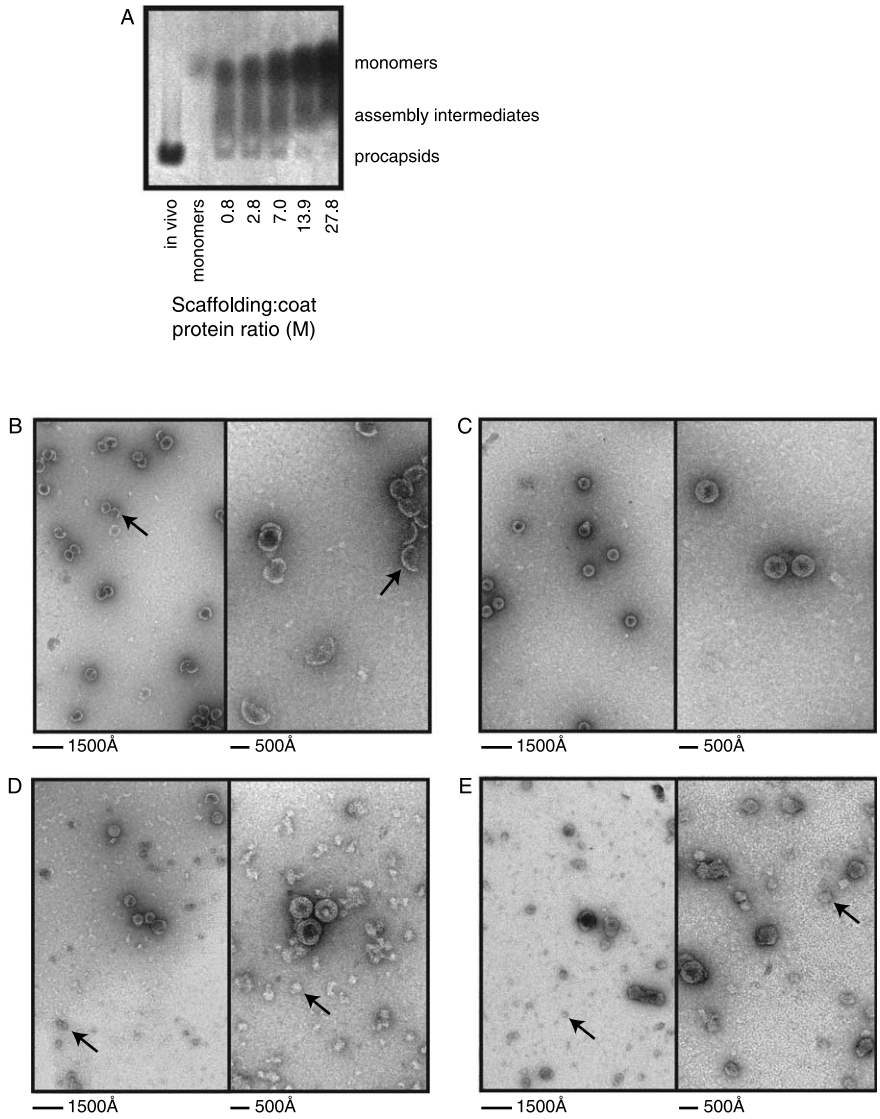

Figure 5. Increasing the concentration of scaffolding protein inhibits assembly. (a) Assembly reactions were done with coat protein held constant at 10.7 μM and scaffolding protein molar ratios as indicated. Samples of each reaction were run on an agarose gel. Up to a molar ratio of 7 scaffolding:coat protein, some complete procapsids were generated. When ratios were above $> \sim 7$, aberrant assembly intermediates were generated. The lane containing monomers refers to coat protein at 10.7 μM; neither intermediates, nor procapsids were present in this sample. The amount of monomer increases with increasing molar ratios of scaffolding protein because unassembled coat protein and scaffolding protein migrate in the same place, as indicated on the right side of the gel. Electron micrographs of negatively stained samples of (b) partial capsids generated without additional NaCl,[12] and molar input ratios of (c) 0.8, (d) 7.0, and (e) 27.8 are shown. Whole procapsids are observed in (c). In (d) and (e) assembly intermediates are seen. Arrows in (d) and (e) indicate examples of assembly intermediates. In (b), arrows point to partial capsids.

procapsids at increasing scaffolding:coat protein ratios with coat protein held at 10.7 μM. An aliquot of each reaction was run on an agarose gel to visualize the products of assembly (Figure 5(a)). When the ratio was greater than 7.0, the amount of procapsids decreased. In addition, a band of lower mobility, which corresponded to assembly intermediates increased in intensity at higher ratios. This band does not run in the same position as the partial capsids observed when assembly reactions are done in the absence of additional NaCl[12] (data not shown). In Figure 5(b)–(e), negative stain electron micrographs of several assembly reactions are shown. Figure 5(b) shows partial capsids generated without NaCl, while Figure 5(c)–(e) show the products of assembly with increasing scaffolding protein, from 0.8 M ratio (Figure 5(c)), which gives normal procapsids, to 27.8 M scaffolding:coat protein ratio, which shows many assembly intermediates that are smaller, more numerous, and distinct in morphology, than the partial capsids shown in Figure 5(b). Electron micrographs were taken of the monomeric subunits and no species that looked like the assembly intermediates, or aggregates, were observed (data not shown). At high ratios, scaffolding protein clearly initiates too

many nuclei causing the formation of distinct assembly intermediates, as we predicted.

Discussion

Weak interactions drive assembly

Previously, Ceres & Zlotnick[5] proposed that capsid assembly could be driven by weak protein–protein interactions. Weak protein–protein interactions were also suggested to be important for thermodynamic editing so that if improper structures are initiated, they could disassemble and allow the subunits to be reused. Here we have shown that each coat protein and scaffolding protein of phage P22 contributes only a small amount of free energy to the procapsid, about −7 kcal/mol per coat protein subunit and about −6 kcal/mol per scaffolding protein subunit. The contributions are in line with those for the subunit interactions of CCMV and HBV, which both are about −7 kcal/mol.[5,13] Because there are so many copies of coat and scaffolding protein, the overall stability of the capsid is large even though the contribution of each protein is small.

Scaffolding protein is found within procapsids in two states: approximately 60 tightly bound scaffolding proteins and the rest which are loosely bound.[37,40] The ΔG value for the tightly bound scaffolding proteins was determined previously to be about −9.0 kcal/mol ($K_d = \sim$100–300 nM), but these investigators could not measure the ΔG value for the more loosely bound scaffolding proteins.[41] This binding energy is an upper limit for the energy each scaffolding protein can contribute to assembly and would be around 540 kcal/mol for a procapsid. We have measured the average contribution of scaffolding protein to procapsid stability. *In vivo*, about 150–350 scaffolding proteins are found in procapsids,[19,43,44] which is consistent with the numbers found in our *in vitro* assembly reactions. Thus, the loosely bound scaffolding proteins outnumber the tightly bound scaffolding proteins. Our data suggest that the loose scaffolding proteins contribute significantly to the stability of procapsids, from around ∼−350 kcal/mol to ∼−1560 kcal/mol procapsid when from 150 to 350 scaffolding proteins are incorporated, explaining why loosely bound scaffolding proteins are included during assembly.

Scaffolding protein concentration is important for assembly

In a normal phage P22 infection *in vivo*, the concentration of free scaffolding protein is around 27 μM and total concentration is around 55 μM.[45] The total intracellular concentration includes scaffolding protein found transiently in procapsids, before DNA packaging occurs. In contrast, the coat protein concentration ultimately reaches over 400–500 μM within the infected cell producing approximately 400 phage/cell. Though coat protein and scaffolding protein are in the same operon, and regulated by only a single promoter, scaffolding protein autogenously modulates its own translation so that the total scaffolding protein concentration is low compared to coat protein.[46] Each scaffolding protein is recycled about five to six times during an infection.[44] Other viruses proteolyze their scaffolding proteins so there is never a large intracellular concentration.[47–49]

Why do viruses so carefully regulate scaffolding protein levels during infection? Under the protein concentrations used for the analysis of ΔG_{PC}, scaffolding protein is mostly monomeric based on the work by Parker *et al.*[50] We chose these concentrations to match the physiological conditions described above. Our data indicate that the optimal concentration of scaffolding protein is important for proper procapsid assembly. When scaffolding:coat protein ratios are too low, the yield of assembly products is low. When scaffolding protein levels are too high, where scaffolding protein will be mostly in a higher-order association, too many nuclei form so that coat protein becomes limiting for the reaction. *In vitro*, these conditions lead to formation of aberrant assembly intermediates and represent a kinetic trap for assembly.[12] *In vivo*, then, it would be crucial for viruses that use a scaffolding protein to regulate the intracellular concentration to achieve a good infection.

The thermodynamic-kinetic model can be used for capsids with more than one protein species

Minimal assumptions are made in the virus-specific thermodynamic-kinetic model.[33] In the model, the reactions are assumed (and have been shown for phage P22) to reach equilibrium.[31] The interactions contributed by capsid proteins are considered equivalent at all times in the reaction; that is for phage P22, all coat protein interactions were treated equally, as were all the interactions for scaffolding protein, yielding an average association energy. The nucleus, which is only critical in kinetic simulations,[9] is assumed to be assembled one subunit at a time, similar to Matsudaira's observation of actin nucleation.[51] The forward microscopic rates are also considered to be equivalent except for the nucleation rates, which can be determined independently.

Here we have shown that this model can be easily applied to a system where two proteins are required for assembly. The predictions made for assembly reactions at equilibrium (e.g. pseudo-critical concentration, weak association energy, and thermodynamic linkage demonstrated by the linear relationship between stability and scaffolding protein content) are demonstrated experimentally in this more complicated system. The model should be readily adaptable to even more complex systems

to understand the function of other capsid proteins in virus assembly reactions.

Materials and Methods

Chemicals, buffers and proteins

Ultrapure urea was purchased from ICN. All other chemicals were reagent grade and purchased from common sources. Purification of coat protein was done as described.[52,53] All experiments described below were done in 20 mM sodium phosphate, 50 mM NaCl buffer, made using Na_2HPO_4, with the pH adjusted to pH 7.6 with H_3PO_4.

Refolded coat protein monomers

Coat protein monomers were obtained from urea-denatured empty procapsid shells, as described, using dialysis at 4 °C against 20 mM sodium phosphate buffer (pH 7.6).[54–56] Coat protein monomers obtained in this way are assembly competent but will not assemble into procapsids until the addition of scaffolding protein.[29,38,52,53,57,58] Monomers were centrifuged at 175,000*g* at 4 °C for 20 min to remove any aggregated or associated structures prior to assembly.

Assembly reactions

To assemble procapsids, refolded coat protein monomers at final concentrations ranging 0.3–0.9 mg/ml (~6.5–19 μM) were mixed with scaffolding protein. The lower limit of the coat protein concentration was set by the pseudo-critical concentration for assembly; that is, below ~6.5 μM coat protein, assembly does not proceed;[37] the upper limit was determined by the solubility of monomeric coat protein (~25 μM) and the required dilution of the proteins. The scaffolding protein was added at concentrations corresponding to molar ratios ranging from 0.28 to 2.8 for a total of 50 reactions, i.e. for the ratio of 2.8, sample one contained coat protein at 0.3 mg/ml (~6.5 μM) and scaffolding protein at 0.6 mg/ml (~18 μM), sample two contained coat protein at 0.4 mg/ml (~8.5 μM) and scaffolding protein at 0.8 mg/ml (~24 μM), etc. Assembly reactions were performed in 20 mM sodium phosphate (pH 7.6), 50 mM NaCl and incubated at 20 °C for >20 h in a total volume of 125 μl.

Analysis of equilibrated assembly reactions

Assembly reactions described above were applied to a 15 ml Sepharose 4B column run at a flow rate of 0.5 ml/min at room temperature in 20 mM sodium phosphate, 50 mM NaCl buffer. Samples of each fraction were then run on SDS-(10%) gels. The gels were silver stained[59] and coat and scaffolding protein bands were quantified using a Kodak EDAS system. The response of the silver stain was linear for the range of protein concentrations used in these experiments (data not shown). Since the yield from the column was greater than 90–95%, the fraction of scaffolding or coat protein was simply calculated from the total of each protein applied to the column. These data were analyzed to determine ΔG_{PC} as described in Results. In Figure 2(b), data were fit with a rectangular hyperbola in the form of:

$$Y = \frac{\text{min \# scaffolding proteins} + (\text{max \# scaffolding proteins} \times Z \times \text{molar input ratio})}{1 + (Z \times \text{input ratio})}$$

where Z is a unitary association constant of scaffolding protein for procapsids that scales the ratio of bound to the ratio of input scaffolding protein.

Agarose electrophoresis

Agarose gels were prepared and run as described.[60,61] In brief, the samples for the native agarose gels were prepared by combining a portion of the assembly reactions with agarose gel sample buffer and loaded onto 1.2% (w/v) Seakem HGT agarose gel. The gels were run at 50 V constant for ~5 h at 4 °C. The agarose gels were stained with Coomassie blue.

Negative stain electron microscopy

A portion of some assembly reactions were used for negative stain electron microscopy (EM). The samples were spun in a microfuge at maximum speed for 5 min to remove any debris. Three microliters of the sample was allowed to absorb to the carbon-coated grid for 1 min. Two to three drops of water were used to wash the grid. The sample was stained with two to three drops of 1% (w/v) aqueous uranyl acetate for 30 s. The excess liquid was wicked off and the grid air-dried. The samples were viewed using a Philips model 300 at 80 kV with magnifications of both 43,400× and 87,400×.

Acknowledgements

We thank Dr Marie Cantino for use of the University of Connecticut Electron Microscopy Center and her expert guidance in electron microscopy. This work was supported by PHS grant GM53567 (to C.M.T.), a PHS fellowship, GM073598 (to K.N.P.), and a University of Connecticut Research Foundation Grant. A.Z. was supported by PHS EB00432.

References

1. Liddington, R. C., Yan, Y., Moulsi, J., Sahli, R., Benjamin, T. L. & Harrison, S. C. (1991). Structure of simian virus 40 at 3.8-Å resolution. *Science*, **354**, 278–284.
2. Rueckert, R. R. (1991). Ricornoviridae and their replication. In *Fundamental Virology* (Fields, B. N. & Knipe, D. M., eds), pp. 409–450, Raven Press, Ltd, New York.
3. Newcomb, W. W. & Brown, J. C. (1991). Structure of herpes simplex virus capsid, effects of extraction with guanidine hydrochloride and partial reconstitution of extracted capsids. *J. Virol.* **65**, 613–620.
4. Fuller, M. T. & King, J. (1980). Regulation of coat protein polymerization by the scaffolding protein of bacteriophage P22. *Biophys. J.* **32**, 381–401.

5. Ceres, P. & Zlotnick, A. (2002). Weak protein–protein interactions are sufficient to srive assembly of Hepatitis B virus capsids. *Biochemistry*, **41**, 11525–11531.
6. Teschke, C. M., King, J. & Prevelige, P. E., Jr (1993). Inhibition of viral capsid assembly by 1,1′-bi(anilino-naphthalene-5-sulfonic acid). *Biochemistry*, **32**, 10658–10665.
7. Zlotnick, A. (2003). Are weak protein–protein interactions the general rule in capsid assembly? *Virology*, **315**, 269–274.
8. Zlotnick, A. (1994). To build a virus capsid. An equilibrium model of the self assembly of polyhedral protein complexes. *J. Mol. Biol.* **241**, 59–67.
9. Zlotnick, A., Johnson, J. M., Wingfield, P. W., Stahl, S. J. & Endres, D. (1999). A theoretical model successfully identifies features of hepatitis B virus capsid assembly. *Biochemistry*, **38**, 14644–14652.
10. Berger, B., Shor, P. W., Tucker-Kellogg, L. & King, J. (1994). Local rule-based theory of virus shell assembly. *Proc. Natl Acad. Sci. USA*, **91**, 7732–7736.
11. Schwartz, R., Shor, P. W., Prevelige, P. E., Jr & Berger, B. (1998). Local rules simulation of the kinetics of virus capsid self-assembly. *Biophys. J.* **75**, 2626–2636.
12. Parent, K. N., Doyle, S. M., Anderson, E. & Teschke, C. M. (2005). Electrostatic interactions govern both nucleation and elongation during phage P22 procapsid assembly. *Virology*, **340**, 33–45.
13. Johnson, J. M., Tang, J., Nyame, Y., Willits, D., Young, M. J. & Zlotnick, A. (2005). Regulating self-assembly of spherical oligomers. *Nano Letters*, **5**, 765–770.
14. Ceres, P., Stray, S. J. & Zlotnick, A. (2004). Hepatitis B virus capsid assembly is enhanced by naturally occurring mutation F97L. *J. Virol.* **78**, 9538–9543.
15. King, J., Botstein, D., Casjens, S., Earnshaw, W., Harrison, S. & Lenk, E. (1976). Structure and assembly of the capsid of bacteriophage P22. *Phil. Trans. Roy. Soc. ser. B*, **276**, 37–49.
16. Prevelige, P. E., Jr & King, J. (1993). Assembly of bacteriophage P22: a model for ds-DNA virus assembly. *Prog. Med. Virol.* **40**, 206–221.
17. Earnshaw, W. & King, J. (1978). Structure of phage P22 coat protein aggregates formed in the absence of the scaffolding protein. *J. Mol. Biol.* **126**, 721–747.
18. Thuman-Commike, P. A., Greene, B., Malinski, J. A., King, J. & Chiu, W. (1998). Role of the scaffolding protein in P22 procapsid size determination suggested by $T=4$ and $T=7$ procapsid structures. *Biophys. J.* **74**, 559–568.
19. Parent, K. N., Ranaghan, M. J. & Teschke, C. M. (2004). A second site suppressor of a folding defect functions *via* interactions with a chaperone network to improve folding and assembly *in vivo*. *Mol. Microbiol.* **54**, 1036–1054.
20. Casjens, S., Adams, M. B., Hall, C. & King, J. (1985). Assembly-controlled autogenous modulation of bacteriophage P22 scaffolding protein gene expression. *J. Virol.* **53**, 174–179.
21. Hoffman, B. & Levine, M. (1975). Bacteriophage P22 virion protein which performs an essential early function. II. Characterization of the gene 16 function. *J. Virol.* **16**, 1547–1559.
22. Hoffman, B. & Levine, M. (1975). Bacteriophage P22 virion protein which performs an essential early function. I. Analysis of 16-ts mutants. *J. Virol.* **16**, 1536–1546.
23. Thomas, D. & Prevelige, P., Jr (1991). Pilot protein participates in the initiation of P22 procapsid assembly. *Virology*, **182**, 673–681.
24. Greene, B. & King, J. (1996). Scaffolding mutants identifying domains required for P22 procapsid assembly and maturation. *Virology*, **225**, 82–96.
25. Bazinet, C. & King, J. (1988). Initiation of P22 procapsid assembly *in vivo*. *J. Mol. Biol.* **202**, 77–86.
26. Earnshaw, W., Casjens, S. & Harrison, S. C. (1976). Assembly of the head of bacteriophage P22: X-ray diffraction from heads, proheads and related structures. *J. Mol. Biol.* **104**, 387–410.
27. Prasad, B. V. V., Prevelige, P. E., Jr, Marieta, E., Chen, R. O., Thomas, D., King, J. & Chiu, W. (1993). Three-dimensional transformation of capsids associated with genome packaging in a bacterial virus. *J. Mol. Biol.* **231**, 65–74.
28. Botstein, D., Waddell, C. H. & King, J. (1973). Mechanism of head assembly and DNA encapsulation in *Salmonella* phage P22. I. Genes, proteins, structures and DNA maturation. *J. Mol. Biol.* **80**, 669–695.
29. Fuller, M. T. & King, J. (1981). Purification of the coat and scaffolding protein from procapsids of bacteriophage P22. *Virology*, **112**, 529–547.
30. King, J., Lenk, E. V. & Botstein, D. (1973). Mechanism of head assembly and DNA encapsulation in *Salmonella* phage P22 II. Morphogenetic pathway. *J. Mol. Biol.* **80**, 697–731.
31. Prevelige, P. E., Jr, Thomas, D. & King, J. (1993). Nucleation and growth phases in the polymerization of coat and scaffolding subunits into icosahedral procapsid shells. *Biophys. J.* **64**, 824–835.
32. Oosawa, F. & Asakura, S. (1975). *Thermodynamics of the Polymerization of Protein*, Academic Press, New York.
33. Zlotnick, A. (2005). Theoretical aspects of virus capsid assembly. *J. Mol. Recognit.* **18**, 479490.
34. Endres, D. & Zlotnick, A. (2002). Model-based analysis of assembly kinetics for virus capsids or other spherical polymers. *Biophys. J.* **83**, 1217–1230.
35. Zlotnick, A., Aldrich, R., Johnson, J. M., Ceres, P. & Young, M. J. (2000). Mechanism of capsid assembly for an icosahedral plant virus. *Virology*, **277**, 450–456.
36. Casini, G., Graham, D., Heine, D., Garcea, R. & Wu, D. (2004). *In vitro* papillomavirus capsid assembly analyzed by light scattering. *Virology*, **325**, 320–327.
37. Teschke, C. M. & Fong, D. G. (1996). Interactions between coat and scaffolding proteins of phage P22 are altered *in vitro* by amino acid substitutions in coat protein that cause a cold-sensitive phenotype. *Biochemistry*, **35**, 14831–14840.
38. Prevelige, P. E., Jr, Thomas, D. & King, J. (1988). Scaffolding protein regulates the polymerization of P22 coat subunits into icosahedral shells *in vitro*. *J. Mol. Biol.* **202**, 743–757.
39. Parker, M. H., Casjens, S. & Prevelige, P. E., Jr (1998). Functional domains of bacteriophage P22 scaffolding protein. *J. Mol. Biol.* **281**, 69–71.
40. Greene, B. & King, J. (1994). Binding of scaffolding subunits within the P22 procapsid lattice. *Virology*, **205**, 188–197.
41. Parker, M. H., Brouillette, C. G. & Prevelige, P. J. (2001). Kinetic and calorimetric evidence for two distinct scaffolding protein binding populations within the bacteriophage P22 procapsid. *Biochemistry*, **40**, 8962–8970.
42. Wyman, J. & Gill, S. (1990). *Binding and Linkage: Functional Chemistry of Biological Macromolecules*, University Science Books, Mill Valley, CA.
43. King, J., Hall, C. & Casjens, S. (1978). Control of the synthesis of phage P22 scaffolding protein is coupled to capsid assembly. *Cell*, **15**, 551–560.

44. Casjens, S. & King, J. (1974). P22 morphogenesis. I: catalytic scaffolding protein in capsid assembly. *J. Supramol. Struct.* **2**, 202–224.
45. Wyckoff, E. & Casjens, S. (1985). Autoregulation of the bacteriophage P22 scaffolding protein gene. *J. Virol.* **53**, 192–197.
46. Casjens, S. & Adams, M. B. (1985). Post-transcriptional modulation of bacteriophage P22 scaffolding protein gene expression. *J. Virol.* **53**, 185–191.
47. Dokland, T. (1999). Scaffolding proteins and their role in viral assembly. *Cell. Mol. Life Sci.* **56**, 580–603.
48. Lata, R., Conway, J. F., Cheng, N., Duda, R. L., Hendrix, R. W., Wikoff, W. R. *et al*. (2000). Maturation dynamics of a viral capsid: visualization of transitional intermediate states. *Cell*, **100**, 253–263.
49. Cheng, H., Shen, N., Pei, J. & Grishin, N. V. (2004). Double-stranded DNA bacteriophage prohead protease is homologous to herpesvirus protease. *Protein Sci.* **13**, 2260–2269.
50. Parker, M. H., Stafford, W. F., III & Prevelige, P. E., Jr (1997). Bacteriophage P22 scaffolding protein forms oligomers in solution. *J. Mol. Biol.* **268**, 655–665.
51. Matsudaira, P., Bordas, J. & Koch, M. (1987). Synchrotron X-ray diffraction studies of actin structure during polymerization. *Proc. Natl Acad. Sci. USA*, **84**, 3151–3155.
52. Teschke, C. M. (1999). Aggregation and assembly of phage P22 temperature-sensitive coat protein mutants *in vitro* mimic the *in vivo* phenotype. *Biochemistry*, **38**, 2873–2881.
53. Teschke, C. M. & King, J. (1993). Folding of the phage P22 coat protein *in vitro*. *Biochemistry*, **32**, 10839–10847.
54. Doyle, S. M., Anderson, E., Parent, K. N. & Teschke, C. M. (2004). A concerted mechanism for the suppression of a folding defect through interactions with chaperones. *J. Biol. Chem.* **279**, 17473.
55. Doyle, S. M., Anderson, E., Zhu, D., Braswell, E. H. & Teschke, C. M. (2003). Rapid unfolding of a domain populates an aggregation-prone intermediate that can be recognized by GroEL. *J. Mol. Biol.* **332**, 937–951.
56. Anderson, E. & Teschke, C. M. (2003). Folding of phage P22 coat protein monomers: kinetic and thermodynamic properties. *Virology*, **313**, 184–197.
57. Fuller, M. T. & King, J. (1982). Assembly *in vitro* of bacteriophage P22 procapsids from purified coat and scaffolding subunits. *J. Mol. Biol.* **156**, 633–665.
58. Teschke, C. M. & King, J. (1995). *In vitro* folding of phage P22 coat protein with amino acid substitutions that confer *in vivo* temperature sensitivity. *Biochemistry*, **34**, 6815–6826.
59. Rabilloud, T., Carpentier, G. & Tarroux, P. (1988). Improvement and simplification of low-background silver staining of proteins by using sodium dithionite. *Electrophoresis*, **9**, 288–291.
60. Teschke, C. M., McGough, A. & Thuman-Commike, P. A. (2003). Penton release from P22 heat-expanded capsids suggests importance of stabilizing penton-hexon interactions during capsid maturation. *Biophys. J.* **84**, 2585–2592.
61. Serwer, P. & Pichler, M. E. (1978). Electrophoresis of bacteriophage T7 and T7 capsids in agarose gels. *J. Virol.* **28**, 917–928.

Edited by M. F. Moody

(Received 5 January 2006; received in revised form 10 March 2006; accepted 31 March 2006)
Available online 21 April 2006